ACS APPLIED MATERIALS & INTERFACES
RESEARCH ARTICLE
www.acsami.org

Molecular Layer Deposition of Functional Thin Films for Advanced Lithographic Patterning

Han Zhou[†] and Stacey F. Bent[*,‡]

[†]Department of Chemistry and [‡]Department of Chemical Engineering, Stanford University

Supporting Information

ABSTRACT: Photoresist materials comprise one of the main challenges faced by lithography to meet the requirements of electronic device size scaling. Here we report for the first time the use of molecular layer deposition (MLD) to produce photoresist materials with controllable placement of functional moieties. Polyurea resists films are deposited by MLD using urea coupling reactions between 1,4-phenylene diisocyanate (PDIC) and ethylenediamine (ED) or 2,2′-(propane-2,2-diylbis(oxy))diethanamine (PDDE) monomers in a layer-by-layer fashion with a linear growth rate, allowing acid-labile groups to be incorporated into the film at well-controlled positions. The films are deposited with stoichiometric compositions and have highly uniform surface morphology as investigated using atomic force microscopy. We show that acid treatment can cleave the backbone of the polyurea film at positions where the acid-labile groups are embedded. We further show that after soaking the polyurea film with photoacid generator (PAG), it acts as a photoresist material and we present several UV patterning demonstrations. This approach presents a new way to make molecularly designed resist films for lithography.

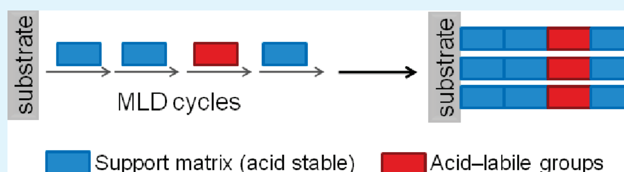

KEYWORDS: molecular layer deposition (MLD), organic film, acid-labile group, photoresist, polyurea

INTRODUCTION

The tremendous progress in micro- and nanoelectronics has been driven in large part by the rapid development of new materials and of new material fabrication techniques. The availability of fabrication methods with atomic or molecular scale control is of particular importance in accelerating performance enhancement for each new generation of electronic devices. One of the key challenges in next-generation electronic devices is the ability to shrink feature sizes, which in turn is driven by improvements in the exposure tools and photoresist materials used in lithography. For current exposure tools, the state-of-the-art is deep ultraviolet (DUV) lithography with immersion and double-patterning.[1] Extreme ultraviolet (EUV) lithography, the most promising next generation lithographic technique, is expected to be introduced for the printing of feature sizes below 22 nm.[2] On the photoresist side, chemically amplified (CA) photoresists, which consist of a photoacid generator (PAG) blended with polymeric resist resins, are widely used in manufacturing. However, photoresists are facing significant challenges to keep pace with the rapidly shrinking feature sizes and to meet the requirements of next generation lithography. Much research on photoresist materials focuses on addressing the resolution, line-width-roughness (LWR), and sensitivity performance trade-off in the materials.[3] PAG-blended resist polymers can suffer from nonuniform PAG distribution in the resist film, as evident by reports of PAG segregation,[4,5] which in turn may potentially cause high roughness of patterns in regions where the acid concentration is relatively low. Moreover, for next generation lithography, the resist film thickness needs to be less than 50 nm with high homogeneity, so as to minimize optical absorption, achieve sufficient resolution, and prevent pattern collapse.[6] Spin-coating may be not suitable for producing ultrathin and highly homogeneous resist films, since a decrease in coating uniformity[7] and an increase in pinhole defects[8] have been observed as film thickness decreases when using spin-coating. As a result, it is necessary to seek alternative photoresist materials solutions. Here, we demonstrate a novel method for photoresist fabrication using the technique of molecular layer deposition (MLD).

MLD, an analogue to atomic layer deposition (ALD), is an emerging technique for depositing nanoscale organic films. MLD utilizes a series of self-limiting reactions of multifunctional organic molecules sequentially at the substrate and grows organic films in a layer-by-layer fashion.[9,10] However, the number of organic linking reactions that have been used for successful MLD is much smaller than that for reactions in solution phase. The reason is that MLD is carried out in vacuum, which imposes limitations such as the lack of solvent and catalyst. MLD systems based on amide,[11−14] imide,[15−17] and urea[18−20] coupling reactions have been successfully demonstrated, and polyamide, polyimide, and polyurea polymeric thin films have been grown and studied.

MLD allows for exquisite control over organic thin films. First, by using self-saturating reactions in multinary cycles, the film thickness can be controlled at the Angstrom level by the number of cycles applied. Second, similar to ALD, MLD can coat high-aspect-ratio features. In contrast, complicated modifications are needed to spin-coat photoresists on high topography

Received: November 9, 2010
Accepted: January 18, 2011
Published: February 08, 2011

ACS Publications © 2011 American Chemical Society

substrates.[21,22] Third, the chemical composition of the deposited organic thin film can be precisely controlled by MLD. Desired functionalities can be embedded into the films by varying the backbone of every organic monomer and thus adjustment of organic film properties, e.g. designed chemical functionality, can be achieved. Also, specific concentrations and positions of chemical functionalities can be readily controlled in the deposited films by using appropriate choice of monomers and number of doses. Given these advantages, MLD has excellent potential for depositing ultrathin photoresist films with high homogeneity in both morphology and composition. Moreover, vapor-phase MLD has some advantages over traditional solution-phase layer-by-layer (LBL) assembly of polymers. The LBL technique often contains many dipping and rinsing steps which may introduce limitations to practical production. In addition, when coating of high-aspect-ratio features is needed, the LBL technique can be problematic since penetration of precursor molecules from solution is not as good as from vapor. Also, the MLD technique does not require any solvent use and thus can be more environmentally friendly. This study demonstrates the application of MLD to such rationally designed photoresist materials.

In a recent study, we have grown polyurea thin films by MLD using 1,4-phenylene diisocyanate (PDIC) and ethylenediamine (ED), and showed the modification of the backbone by insertion of a sulfide group into the diamine precursor.[20] The urea coupling reaction between isocyanate and amine groups has a high reaction rate and does not form any byproduct, both eliminating the need for a postdeposition annealing step to complete the reaction and preventing side reactions caused by byproduct.[13] A polyurea film was previously used as a negative-tone photoresist material by Sato and co-workers.[23] In that work, aromatic polyurea films with thicknesses of several hundred nanometers were deposited using vapor deposition polymerization of 4,4′-diphenylmethane diisocyanate and 4,4′-diaminodiphenylmethane. The application of the films as negative-tone photoresists was based on the difference of thermal resistances between UV-exposed and unexposed polyurea. A resolution of 5 μm was achieved. However, patterning of feature sizes smaller than 5 μm failed, probably because the difference in thermal stability was not big enough to achieve small feature sizes, or because cross-linking within the polyurea film during UV exposure or annealing imposes limitations in fine resolution. Here we report on an ultrathin, positive-tone, chemically amplified polyurea photoresist film with acid-labile groups embedded into the backbone and demonstrate its use as a photoresist material. The film is deposited by MLD using 1,4-phenylene diisocyanate (PDIC) and 2,2′-(propane-2,2-diylbis(oxy))diethanamine (PDDE), where the acetal functional group is inserted into the diamine precursor to impart acid lability. We show that this acetal-containing polyurea film is stable in base and labile in acid. We also demonstrate successful patterning of the MLD resist film to a resolution of 4 μm. The ability to pattern this ultrathin polyurea film provides a possible solution for photoresist materials in next generation lithography.

EXPERIMENTAL METHODS

The reactor used to deposit MLD films is a hot wall flow reactor heated by external heating tapes that are controlled by variable transformers. A Leybold Trivac rotary vane pump is used to pump the reactor which has a base pressure below 1 mTorr, as monitored by a convectron gauge. MLD precursors and nitrogen purge gas were introduced into the reactor using manually actuated valves.

3-Aminopropyltriethoxysilane (APTES), 1,4-phenylene diiscocyanate (PDIC), ethylenediamine (ED), triphenylsulfonium triflate (TPSOTf), and propylene glycol methyl ether acetate (PGMEA) were purchased from Sigma Aldrich and used as received. 37% hydrochloric acid (HCl) and 25 wt % tetramethylammonium hydroxide (TMAH) aqueous solution were also purchased from Sigma Aldrich and diluted in H_2O to the desired concentrations. 2,2′-(propane-2,2-diylbis(oxy))-diethanamine (PDDE) was synthesized using the method reported in the literature.[24] The PDDE is an amber-colored viscous liquid. Spectroscopic characteristics are consistent with those reported in the literature.[24] NMR measurement shows that the purity of the PDDE product is 92%, with 2-propanol used in the synthesis as the major impurity. Films were deposited on silicon (100) wafers. The silicon wafers were cleaned before MLD with piranha cleaning solution followed by an APTES initial surface functionalization using a process reported in the literature[25] and described in detail in our previous study.[20] Each complete PDIC/PDDE MLD cycle consists of a 10-min PDIC dose, followed by purging with nitrogen gas for 2 min, and then a 5-min PDDE dose, followed by purging with nitrogen gas for 4 min. The deposition conditions for the PDIC/ED MLD cycles are similar, except that the dosing time for the ED precursor is 2 min and the purging time after the ED dose is 5 min. To deposit PDIC/ED/PDDE laminates,we replaced the ED dose with the PDDE dose at specific cycles. PDIC was heated in a silicone oil bath with a temperature between 60 and 65 °C, at which temperature PDIC can be sublimed.[26] PDDE and ED are liquids and were kept at room temperature. The MLD depositions were performed at room temperature. Sufficient PDIC vapor delivery to silicon wafers was achieved despite possible condensation of PDIC on the chamber walls because the PDIC bath temperature was higher than the deposition temperature. The dosing procedure for PDIC, PDDE, and ED was to keep the valves to the sample vials open while isolating the reactor from the pump; in the case of ED, once the reactor pressure reached 1 Torr, the valve to the sample was closed. Samples were taken out of the reactor for ex situ analysis and characterization after MLD.

To incorporate the triphenylsulfonium triflate PAG, the PDIC/PDDE films were immersed into a saturated solution of TPSOTf in propylene glycol methyl ether acetate (PGMEA) for 20 min and the PGMEA solvent was blown dry with compressed air. For rough pattern-
ing, the polyurea resist film was exposed to a 254 nm UV lamp (ozone-free, double bore lamp, model 82−3309−2, Jelight Company Inc. Irvine, CA, USA) through a grid mask. For fine patterning, a Karl Suss MA6 aligner with an i-line (365 nm) UV light source was used for exposure. After exposure to either source, samples underwent postexposure bake (PEB) on a hot plate with a temperature between 90 and 100 °C for 1 to 5 min, then were developed in 0.26 M aq. TMAH solution, rinsed with deionized (DI) water, and finally blown dry using compressed air.

A Gaertner Scientific Corp. L116C He−Ne laser ellipsometer with 632.8 nm light was used for ellipsometry measurements. The sample thickness was measured in at least 3 different locations on each sample so as to test film uniformity across it. A refractive index of 1.46 was used for both the SiO_2 and organic film, because the refractive indices of both materials are very close.[27−29] The SiO_2 thickness of piranha-cleaned silicon samples was measured, used as a baseline oxide thickness, and subtracted from the subsequent total film thickness values to yield the thickness of the organic film deposited above the SiO_2 layer.

Fourier-transform infrared (FTIR) spectroscopy measurements were performed on a Thermo Nicolet 6700 FT-IR spectrometer using a MCT-A detector in the transmission mode. Spectra were taken with 200 scans at 4 cm^{-1} resolution. Piranha-cleaned silicon samples were used as a background reference.

X-ray photoelectron spectroscopy (XPS) was performed on a Surface Science Instruments S-Probe spectrometer and a Physical Electronics, Inc. 5000 Versaprobe spectrometer. Both spectrometers used Al Kα

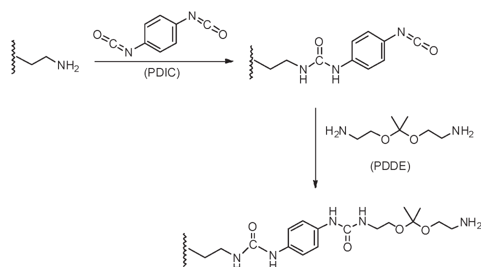

Figure 1. MLD scheme with PDIC and PDDE precursors on an APTES-coated surface.

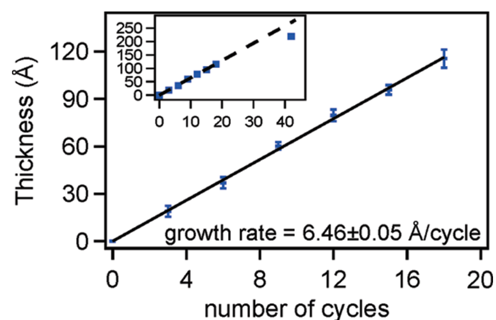

Figure 2. Plot of polyurea film thickness as a function of number of MLD cycles. The inset includes a film thickness of 22 nm for a 42-cycle PDIC/PDDE MLD film.

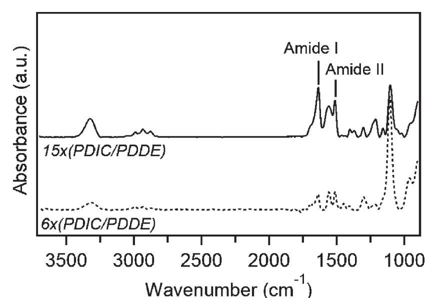

Figure 3. FTIR spectra of PDIC/PDDE polyurea films after 6 and 15 MLD cycles.

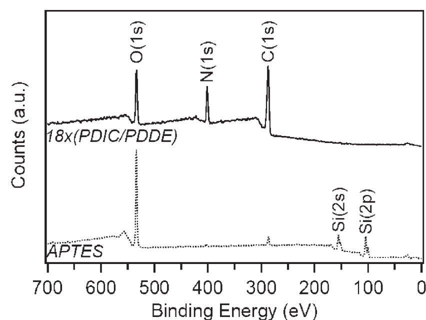

Figure 4. X-ray photoelectron spectroscopy survey scans for the APTES-modified surface and an 18-cycle PDIC/PDDE film.

radiation (1486.6 eV) as the excitation source. Survey scans were performed to measure the elemental composition of each sample using an energy step of 1 eV, and fine scans were performed to investigate binding energy shifts and chemical environments of the elements using a step size of 0.1 eV. Atomic compositions were calculated by determining peak area integrals, and peaks were fit using Gaussian profiles with a Shirley background. Multiple peaks within a single fine scan were fit by constraining the peak full-widths at half-maximum to be identical.

Film surface morphology was measured on a Park XE-70 Atomic Force Microscope (AFM) using silicon nitride tips in a tapping mode. Line scans of elemental composition across lithographic feature were performed using Auger electron spectroscopy (AES) on a Physical Electronics, Inc. 700Xi Auger Nanoprobe. Images of the lithographic patterns were taken by an FEI XL30 Sirion scanning electron microscope (SEM) with a secondary electron detector.

RESULTS AND DISCUSSION

Figure 1 represents the MLD scheme for deposition of polyurea thin films with acetal groups in the backbone. After piranha solution cleaning, the silicon wafers were coated with a monolayer of APTES via silanization between ethoxy groups of APTES and hydroxyl groups on the SiO_2 substrate surface, leaving the surface terminated with amine groups for subsequent reaction. Subsequently, the PDIC monomers were introduced into the reactor, where they reacted with the amine groups and left an isocyanate-terminated surface, which in turn reacted with PDDE precursors dosed in the next step. A single MLD cycle consisted of the two-step doses of PDIC and PDDE and was repeated until a desired film thickness was obtained.

Polyurea thin films were deposited with various numbers of MLD cycles. Film thicknesses measured by ellipsometry are plotted in Figure 2. The data in Figure 2 show that film thickness has a linear dependency on the number of MLD cycles, with a constant growth rate of 6.46 ± 0.05 Å per cycle. This growth rate is slightly higher than that of PDIC/ED polyurea films,[20] agreeing with the longer molecular length of the PDDE monomer than the ED monomer. The molecular chain length of each PDIC/PDDE unit is about 18 Å, suggesting either that the polymer chains are tilted at an angle of 68° from the surface normal or that submonolayer coverage is formed at each cycle during the deposition. However, the exact microstructure of the MLD film can not be obtained merely from these data, and further study is needed for elucidation.

To investigate the chemical bonding in the PDIC/PDDE film, we carried out FTIR spectroscopy measurements. Figure 3 shows the FTIR spectra of PDIC/PDDE MLD films after 6 and 15 cycles. Comparing the two spectra, all peaks increased from 6 to 15 MLD cycles. We note that the ν(C−H) absorptions (2950−2800 cm^{-1}) are sensitive to adventitious carbon obtained during the ex-situ analysis and cannot be used for quantitative comparison. Among the IR peaks, the most important ones are ν(N−H) at 3310 cm^{-1}, ν(C═O) at 1651 cm^{-1}, and δ(N−H) at 1510 cm^{-1}. The ν(C═O) and δ(N−H) peaks are characteristic amide I and amide II modes of urea,[30] strongly supporting that the films are built by urea coupling reactions between isocyanate and amine groups.

XPS spectra, as shown in Figure 4, were obtained to check the chemical composition of the PDIC/PDDE MLD film. Comparing the spectrum taken after 18 cycles of PDIC/PDDE MLD to the one taken after the initial APTES surface modification shows that carbon and nitrogen signals increased significantly and the silicon signal from the underlying SiO_2 substrate disappeared, agreeing with successful deposition of the organic film. The ideal atomic ratio of C/N/O for the PDIC/PDDE polyurea film is 3.75/1/1, and the experimental ratio calculated from the XPS

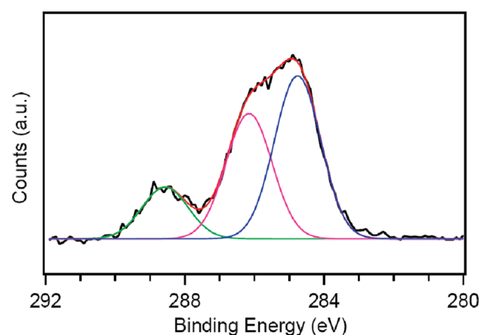

Figure 5. X-ray photoelectron C (1s) fine scan spectra of for an 18-cycle PDIC/PDDE film.

spectra is 4.32 ± 0.21/1/1.16 ± 0.07. The small discrepancy comes from a small amount of adventitious carbon and a small amount of oxygen signal from the underlying SiO_2 substrate. The elemental XPS fine scans reveal information about the atomic environments and chemical bonding in the film. Figure 5 shows a fine scan of the C (1s) XPS signal in a PDIC/PDDE film. At least three peaks are discernible: peaks at 288.6, 286.2, and 284.8 eV. Because the binding energy increases as the electron density of the carbon atom decreases, the peak at 288.6 eV is assigned to the carbonyl carbons in the urea linkage; the peak at 286.2 eV corresponds to alkyl carbons and the peak at 284.8 eV results from aromatic carbons.[31] This result agrees well with our expectation, because the urea linkages contains carbonyl carbons and the PDDE and PDIC precursors introduce alkyl and aromatic carbons, respectively. The experimental ratio of carbonyl/alkyl/aromatic carbons is 1/2.2/2.9, and the theoretical value is 1/3.5/3. The discrepancy again likely lies with uptake of adventitious carbon after the film was grown.

Atomic force microscopy (AFM) was carried out to study the surface morphology of the PDIC/PDDE polyurea films. For a 42-cycle PDIC-PDDE film with a thickness of 22 nm, as measured by ellipsometry, the rms roughness (R_q) measured by AFM is only 0.1 nm, indicating a uniform organic film coating over the substrate. However, the growth rate of 6.46 Å/cycle measured in the linear film growth experiment is higher than the value of 5.24 Å/cycle observed for this sample, as shown in the inset of Figure 2. The higher growth rate likely resulted from the frequent vacuum breaks in the growth rate measurement experiment: when samples are retrieved from the vacuum chamber, analyzed and then replaced into the vacuum chamber for further MLD cycles, some ambient contaminants may adsorb onto the sample and lead to a higher apparent growth rate.

To function as a positive-tone photoresist material, it is necessary for the PDIC/PDDE film to be stable in the developer (a basic solution) and to dissolve upon exposure to acid. To test the lability in acid and stability in basic developer, we immersed two 18-cycle PDIC/PDDE films in 0.2 M aq. hydrochloric acid (HCl) solution and 0.26 M aq. tetramethylammonium hydroxide (TMAH) solution for 3 min with slight agitation, respectively. Before any measurements, both films were rinsed with DI water and blown dry in compressed air after the acid or base treatment. The changes of the films were investigated by FTIR spectroscopy and XPS, and the results are shown in Figures 6 and 7, respectively. The PDIC/PDDE film is clearly stable in TMAH solution, as barely any change in chemical bonding or elemental composition could be observed. Both FTIR (Figure 6b) and XPS (Figure 7b) spectra taken after the base treatment are almost

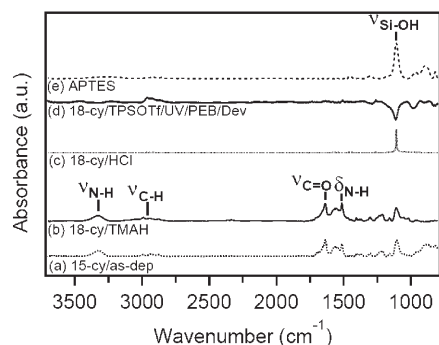

Figure 6. FTIR spectra of PDIC/PDDE films: (a) 15-cycle film, as-deposited; (b) 18-cycle film, after TMAH treatment; (c) 18-cycle film, after HCl treatment; (d) 18-cycle film, soaked with TPSOTf, exposed to UV light and PEB, and developed; (e) APTES-modified surface shown for reference.

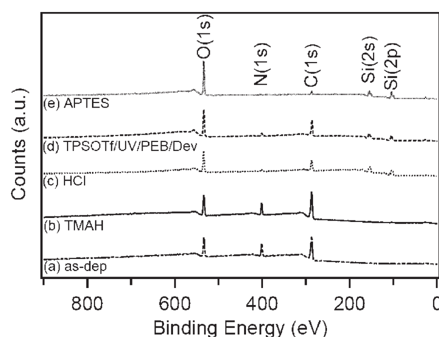

Figure 7. XPS spectra of 18-cycle PDIC/PDDE films: (a) as-deposited; (b) after TMAH treatment; (c) after HCl treatment; (d) soaked with TPSOTf, exposed to UV light and PEB, and developed. (e) APTES-modified surface shown for reference.

identical to those of the as-deposited film (Figures 6a and 7a). In contrast, the PDIC/PDDE film showed strong lability upon acid treatment, where the PDDE component can be decomposed into alcohols and acetone, as shown in Figure 8a. As shown in Figure 6c, the only absorption feature after acid treatment is ν(Si−OH) at 1084 cm^{-1}, which is due to the hydroxylated SiO_2 substrate. The disappearance of the ν(N−H) peak at 3310 cm^{-1}, ν(C═O) peak at 1651 cm^{-1} and δ(N−H) peak at 1510 cm^{-1} suggests that the PDIC/PDDE film is removed under acidic condition. Analysis of the elemental composition by XPS also supports the acid lability of the PDIC/PDDE film. As shown in Figure 7c, after the acid treatment, the N (1s) signal decreased significantly, indicating that the PDIC/PDDE film is removed, since it is the only source of nitrogen besides the initial APTES monolayer. Notably, the N (1s) signal after the acid treatment is stronger than that of the APTES monolayer (Figure 7e) because the first PDIC layer is not acid-cleavable, leaving two molecular urea units above the APTES monolayer, as shown in Figure 8b, and this moiety is not acid cleavable. Meanwhile, both Si (2s) and Si (2p) peaks increased greatly, indicating the removal of deposited film and recovery of the SiO_2 substrate.

An important strength of MLD is to precisely control the composition and functionalities of the deposited film at the subnanometer scale. Taking advantage of this property, we deposited a series of PDIC/ED/PDDE laminated films with various thicknesses of each block to study the tunability of the acid-cleavage

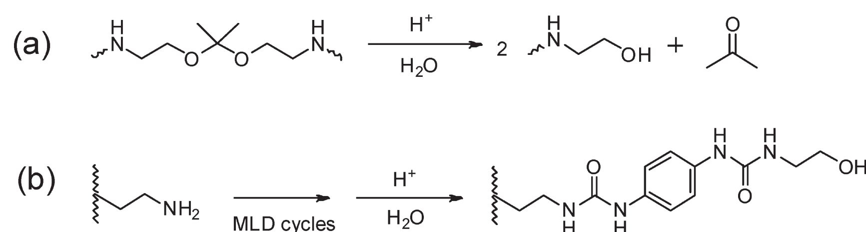

Figure 8. (a) Acid-cleaving reaction in the PDIC/PDDE film that occurs at the PDDE component. (b) Structure of the residue on the surface after acid cleavage of the PDIC/PDDE MLD film.

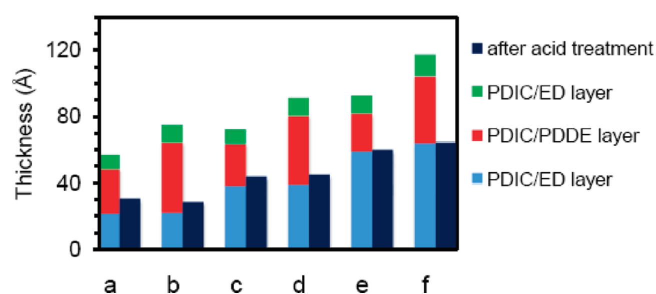

Figure 9. Thicknesses of various PDIC/ED/PDDE laminates before and after acid treatment. The numbers of cycles of the bottom PDIC/ED layer, the middle PDIC/PDDE layer and the top PDIC/ED layer are [3,3,3], [3,6,3], [6,3,3], [6,6,3], [9,3,3], and [9,6,3] for samples a−f, respectively.

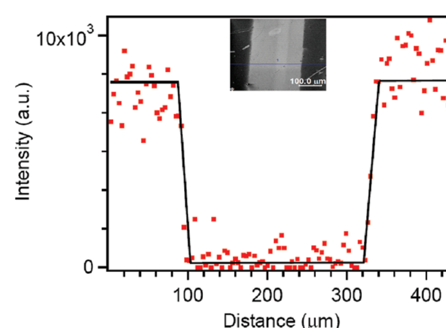

Figure 10. AES line scan of nitrogen across a feature after grid mask patterning (see inset) of a PAG loaded MLD film. The film was deposited by 42 cycles of PDIC/PDDE.

sites in the MLD films. After the initial APTES attachment to the substrate, films of 3, 6, and 9 PDIC/ED cycles were deposited, followed by 3 or 6 PDIC/PDDE cycles and 3 more PDIC/ED cycles at the end. Since urea coupling was maintained as the linking reaction in both PDIC/ED and PDIC/PDDE MLD cycles, alternating the diamine precursor did not interfere with the MLD process. The growth rate was consistent with the sum of the two MLD processes. In these laminates, only the middle block of PDIC/PDDE film is designed to be acid-cleavable, while the top and bottom blocks of PDIC/ED are stable under acidic condition. The acid stability of PDIC/ED films was confirmed via acid treatment in separate studies. After treating a 83 Å thick PDIC/ED film with 1 M aq. HCl solution, we observed only a 12 Å film thickness loss, without any detectable difference in the film chemical composition or chemical bonding, as measured by XPS and FTIR, respectively.

After deposition of various thicknesses of distinctive acid-cleavable and acid-stable blocks, all the samples were immersed in 0.2 M aq. HCl solution for 3 min, followed by rinsing in DI water and drying in compressed air. Results of ellipsometry measurements of the film thicknesses before and after the acid treatment are shown in Figure 9. Comparison of film thicknesses before and after the acid treatment reveals that the laminates cleaved exactly at the positions where acid-labile groups were embedded, demonstrating the capability of controlling positions of desired functionalities.

Because only acid-labile groups are contained in the PDIC/PDDE film after deposition, photoacid generators (PAGs) need to be incorporated into the film to make it a functional photoresist material. To test their behavior as resists, triphenylsulfonium triflate (TPSOTf), a widely used PAG, was soaked into the PDIC/PDDE films. The incorporation of TPSOTf in the PDIC/PDDE film was confirmed by FTIR spectroscopy and XPS measurements, which can be found in the Supporting Information together with the chemical structure of TPSOTf. Importantly, our results also show that the acid generated from TPSOTf under UV radiation can cleave the film, as did HCl. As shown in Figures 6d and 7d, after exposing the PDIC/PDDE film soaked with TPSOTf to UV light under a 254 nm UV lamp and carrying out post exposure bake and development, the film was removed: both amide I and amide II IR peaks disappeared, indicating the loss of the urea linkages. The presence of C−H vibrational absorptions (2950−2800 cm^{-1}) in Figure 6d is attributed to adventitious carbon uptake. Also, loss of N (1s) signal and gain of Si (2s) and Si (2p) signals in the XPS spectrum confirms the efficient removal of the organic film. However, the PDIC/PDDE film was not as completely removed with acid generated by the PAG as it was with direct aqueous acid, according to ellipsometry measurements.

To demonstrate that the MLD film can be used for lithographic patterning, a patterning experiment was performed using a grid mask. A 42-cycle PDIC/PDDE film with a thickness of 25 nm was soaked with TPSOTf, exposed to UV light for 4 min, then subjected to postexposure bake and TMAH development. Figure 10 shows an SEM image of a 230 μm feature of the pattern together with an AES line scan of nitrogen across the feature, showing that the pattern of the grid mask was successfully transferred to the sample. The intensity of the nitrogen signal of the unexposed area (dark area in the SEM image) is much higher than that of the exposed area (bright area in the SEM image), agreeing with our expectation. In addition, the AES line scan shows that the low-nitrogen-content area has a width of 220 μm, which is in good agreement with the SEM image. Moreover, the sharp change of nitrogen intensity in the AES line scan suggests a steep sidewall of the feature.

Finally, a finer scale patterning experiment was performed on an i-line (λ = 365 nm) aligner. As before, a 42-cycle PDIC/PDDE MLD film soaked with TPSOTf was used as the photoresist material.

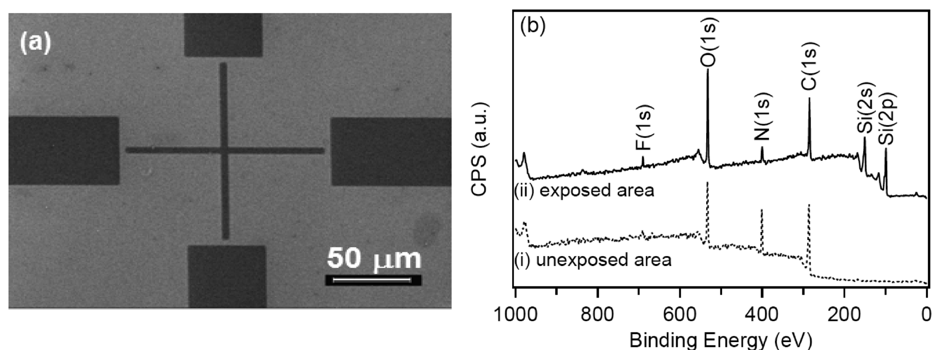

Figure 11. (a) SEM image of substrate after i-line UV patterning. The dark and bright fields correspond to unexposed and exposed area, respectively. (b) XPS survey scans of (i) unexposed and (ii) exposed fields.

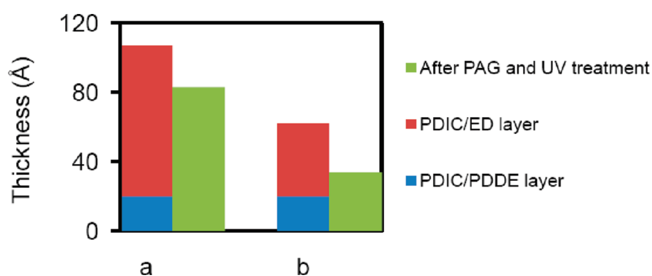

Figure 12. Thicknesses of various PDIC/PDDE/ED laminates immediately after deposition and after treatment of PAG soaking, UV exposure, post exposure bake and development. Sample a was deposited with 3-cycle PDIC/PDDE and 15-cycle PDIC/ED, and sample b was deposited with 3-cycle PDIC/PDDE and 8-cycle PDIC/ED.

After 50 s exposure, 1 min PEB at 90 °C, 1 min development in 0.26 M aq. TMAH developer, rinsing in DI water and air drying, the pattern was well resolved, as shown in the SEM image in Figure 11a, with feature sizes as small as 4 μm. XPS survey scans were performed at both exposed and unexposed fields of the sample to compare the elemental compositions. The result is shown in Figure 11b. The exposed field has a significantly weaker N (1s) signal and stronger Si (2s) and Si (2p) signals, confirming the efficient removal of photoresist material by UV lithographic patterning. The remaining nitrogen in the spectrum of the exposed field is attributed to N in APTES and the first PDIC layer at the surface, as discussed above. It should be noted that the resolution of 4 μm demonstrated here is the smallest feature of the photomask used and not necessararily the limit of the MLD photoresist, as we believe with a finer photomask this resolution can be improved. Moreover, the PAG-soaking technique is not optimized, and improvements in the incorporation of the PAG will lead to further enhancements of the lithographic performance of the novel MLD photoresist materials.

As mentioned earlier, ellipsometric measurements showed that the PDIC/PDDE films were not as fully removed with the PAG as with aqueous acid. The lower efficiency of film removal with the PAG may be due to limitations in the extent of PAG doping achieved with the soaking process or to limitations of the acid diffusion length. However, the diffusion length of the acid generated by the PAG is typically reported to be ~20 nm,[32] which is very close to the thickness of the PDIC/PDDE MLD films. Consequently, we propose that limitations in the spatial extent of the PAG doping is the more likely reason, although there exist other less-likely factors such as airborne contaminants that act as acid quenchers present in the noncleanroom lab environment where most of the experiments were carried out. To examine the PAG doping profile, or the depth at which the PAG (TPSOTf) penetrates the MLD film, we deposited a series of PDIC/PDDE/ED laminates, with 3-cycle PDIC/PDDE acid labile films at the bottom and 8 or 15-cycle PDIC/ED acid stable films at the top. After deposition, the laminates were soaked with TPSOTf, exposed to UV lamp, post exposure baked and developed. The thicknesses of the laminates right after deposition and after the complete treatment were measured by ellisometry and the result is shown in Figure 12. The laminates were not efficiently cleaved after the treatment. The loss of thickness of the laminates after PAG and UV treatment is likely due at least in part to microstructural rearrangement of the MLD polymer chains caused by UV radiation, baking and rinsing, rather than acid cleavage. The inefficient removal of the MLD laminates indicates that the PDIC/ED layer at the top acted as a PAG barrier and the PAG did not fully penetrate the film to reach the bottom PDIC/PDDE layer. Otherwise, the laminates would be cleaved at the bottom PDIC/PDDE layer and more removal of the laminates would be observed. We also tried immersing the PDIC/PDDE MLD films in TPSOTf solutin for 1 h, but the longer immersion time did not enhance the cleavage efficiency of the MLD films. This points out the interesting diffusion properties of the MLD films, as the well-packed MLD layers may not allow dopants to diffuse efficiently, and motivates future studies to investigate this property.

CONCLUSIONS

We have successfully applied molecular layer deposition (MLD) to produce photoresist materials with controllable placement of functional moieties. MLD was used to incorporate acid-labile groups into polyurea films by inserting acetal functionality into the backbone of a diamine monomer and using urea coupling reactions between diamine and diisocyanate precursors. The deposition occurs with a constant growth rate in a layer-by-layer fashion. Urea linkages within the MLD film are confirmed by FTIR spectra, as two key amide vibrational modes were observed. The MLD film has stoichiometric elemental composition and a very uniform surface morphology.

The polyurea MLD film containing acid-labile groups in the backbone are shown to be stable under basic conditions and cleavable under acidic conditions, by both direct aqueous acid exposure and photoacid exposure formed by soaked-in photoacid generator. Moreover, we demonstrate control over the acid-cleaving position in standard/acid-labile polyurea nanolaminates.

The PAG-soaked acid-labile polyurea films were used as a photoresist material, and UV patterning demonstrations are presented. The lithographic performance of this MLD photoresist material is expected to be improved by optimizing the conditions of PAG incorporation into the MLD film.

ASSOCIATED CONTENT

Supporting Information. FTIR and XPS spectra of PDIC/PDDE MLD films soaked with TPSOTf; chemical structure of TPSOTf (PDF). This material is available free of charge via the Internet at http://pubs.acs.org/.

AUTHOR INFORMATION

Corresponding Author
*E-mail: sbent@stanford.edu.

ACKNOWLEDGMENT

We acknowledge support of this work from Intel Corporation. Dr. Todd Younkin and Dr. James Blackwell are gratefully acknowledged for helpful discussions and valuable suggestions about photoresist design and lithographic processing. Paul Loscutoff is thanked for helpful discussions and Zijian Li is thanked for help with the i-line aligner.

REFERENCES

(1) *International Technology Roadmap for Semiconductors: 2009 Lithography Update*. http://www.itrs.net/links/2009Winter/Presentations/Conference/Litho_121609.pdf
(2) Wagner, C.; Harned, N. *Nat. Photonics* **2010**, *4*, 24.
(3) Van Steenwinckel, D.; Lammers, J. H.; Leunissen, L. H.; Kwinten, J. A. J. M. *Proc. SPIE* **2005**, *5753*, 269.
(4) Covert, K. L.; Russell, D. J. *J. Appl. Polym. Sci.* **1993**, *49*, 657.
(5) Fedynyshyn, T. H.; Astolfi, D. K.; Cabral, A.; Roberts, J. *Proc. SPIE* **2007**, *6519*, 65190X.
(6) Jouve, A.; Simon, J.; Foucher, J.; David, T.; Tortai, J.-H.; Solak, H. *Proc. SPIE* **2005**, *5753*, 720.
(7) Walsh, C. B.; Franses, E. I. *Thin Solid Films* **2003**, *429*, 71.
(8) Kuan, S. W. J.; Frank, C. W.; Lee, Y. H. Y.; Eimori, T.; Allee, D. R.; Pease, R. F. W.; Browning, R. *J. Vac. Sci. Technol., B* **1989**, *7*, 1745.
(9) Ritala, M.; Leskela, M. In *Handbook of Thin Film Materials*, Nalwa, H. S., Ed.; Academic Press: San Diego, CA, 2002; Vol. 1.
(10) George, S. M.; Yoon, B.; Dameron, A. A. *Acc. Chem. Res.* **2009**, *42*, 498.
(11) Kubono, A.; Yuasa, N.; Shao, H. L.; Umemoto, S.; Okui, N. *Thin Solid Films* **1996**, *289*, 107.
(12) Shao, H. I.; Umemoto, S.; Kikutani, T.; Okui, N. *Polymer* **1997**, *38*, 459.
(13) Du, Y.; George, S. M. *J. Phys. Chem. C* **2007**, *111*, 8509.
(14) Adarnczyk, N. M.; Dameron, A. A.; George, S. M. *Langmuir* **2008**, *24*, 2081.
(15) Bitzer, T.; Richardson, N. V. *Appl. Phys. Lett.* **1997**, *71*, 1890.
(16) Yoshimura, T.; Tatsuura, S.; Sotoyama, W. *Appl. Phys. Lett.* **1991**, *59*, 482.
(17) Bitzer, T.; Richardson, N. V. *Appl. Surf. Sci.* **1999**, *144*—*45*, 339.
(18) Usui, H. *Thin Solid Films* **2000**, *365*, 22.
(19) Kim, A.; Filler, M. A.; Kim, S.; Bent, S. F. *J. Am. Chem. Soc.* **2005**, *127*, 6123.
(20) Loscutoff, P. W.; Zhou, H.; Clendenning, S. B.; Bent, S. F. *ACS Nano* **2010**, *4*, 331.
(21) Kutchoukow, V. G.; Mollinger,J. R.; Bossche, A. In *Proceedings of 13th European Conference on Solid-State Transducers (Eurosensors XIII)*; Lausanne, Switzerland, Sept 6—9, 1999; EPFL: Lausanne, Switzerland, 1999, pp 256.
(22) Pham, N. P.; Sarro, P. M.; Burghartz, J. N. *Proc. SPIE* **2000**, *4174*, 390.
(23) Sato, M.; IIjima, M.; Takahashi, Y. *J. Photopolym. Sci. Technol.* **1995**, *8*, 137.
(24) Paramonov, S. E.; Bachelder, E. M.; Beaudette, T. T.; Standley, S. M.; Lee, C. C.; Dashe, J.; Frechet, J. M. J. *Bioconjugate Chem.* **2008**, *19*, 911.
(25) Zheng, W. W.; Frank, C. W. *Langmuir* **2010**, *26*, 3929.
(26) Jensen, S.; Früchtl, H.; Baddeley, C. J. *J. Am. Chem. Soc.* **2009**, *131*, 16706.
(27) Vandenberg, E. T.; Bertilsson, L.; Liedberg, B.; Uvdal, K.; Erlandsson, R.; Elwing, H.; Lundstrom, I. *J. Colloid Interface Sci.* **1991**, *147*, 103.
(28) Haller, I. *J. Am. Chem. Soc.* **1978**, *100*, 8050.
(29) Howarter, J. A.; Youngblood, J. P. *Langmuir* **2006**, *22*, 11142.
(30) Vien, D. L.; Colthup, N. B.; Fateley, W. G.; Grasselli, J. G. *The Handbook of Infrared and Raman Characteristic Frequencies of Organic Molecules*; Academic Press: London, 1991.
(31) Beamson, G.; Briggs, D. *High-Resolution XPS of Organic Polymers: The Scienta ESCA300 Database*; Wiley: Chichester, U.K., 1992.
(32) Kim, J. H.; Kim, Y. H.; Chon, S. M.; Nagai, T.; Noda, M.; Yamaguchi, Y.; Makita, Y.; Nemoto, H. *J. Photopolym. Sci. Technol.* **2004**, *17*, 379.